AJRCMB Articles in Press. Published on July 21, 2011 as doi:10.1165/rcmb.2010-0426OC

MATRIX PROTEINS FROM SMOKE EXPOSED FIBROBLASTS ARE PRO-PROLIFERATIVE

David I Krimmer[1,2 *], Janette K Burgess[1,2] , Teh K Wooi[1,2], Judith L Black[1,2] & Brian GG Oliver[1,2]

1. Woolcock Institute of Medical Research - Cell Biology
Sydney, New South Wales
Australia

2. University of Sydney - Pharmacology
Sydney, New South Wales
Australia

*Corresponding Author: David Krimmer. Woolcock Institute of Medical Research, Sydney, Australia, dkri7356@uni.sydney.edu.au

Abstract:

Background: Airway remodeling decreases lung function in chronic obstructive pulmonary disease (COPD). Extracellular matrix (ECM) deposition is increased in remodeled airways and drives cellular processes of proliferation, migration and inflammation. We investigated the role of cigarette smoke in altering the ECM deposited from human lung fibroblasts. Methods: Lung fibroblasts isolated from patients with COPD or other lung disease were exposed to cigarette smoke extract (CSE) and 5ng/ml transforming growth factor (TGF)-β1 for 72 hours, in some experiments inhibitors of signaling molecules were added. Deposition of perlecan, fibronectin and elastin were measured using ELISA. Release of interleukin (IL)-8 and IL-13 were measured using ELISA. Unstimulated fibroblast cells were re-seeded onto deposited matrix and assessed for proliferation and cytokine release. Results: Five percent CSE increased deposition of fibronectin and perlecan from only COPD fibroblasts. Fibronectin and perlecan deposition was attenuated by addition of the NF-κB inhibitor BMS-345541, and the signal transduction and activator of transcription (STAT)-1/3 inhibitor pyridone 6, respectively. Five percent CSE increased IL-8 release from COPD fibroblasts more than non-COPD fibroblasts. This increase was attenuated by BMS-345541. Matrix deposited following 5% CSE stimulation increased proliferation of fibroblasts but did not alter cytokine release. Conclusion: ECM produced from COPD fibroblasts following CSE exposure has pro-proliferative effects. Thus the ECM in patients with COPD may create an environment which promotes airway remodeling.

Introduction

Chronic obstructive pulmonary disease (COPD) is a preventable obstructive disease of the lung caused by inhalation of noxious particles[1]. Prevalence of COPD is increasing and is projected to be the third leading cause of death worldwide by 2020[2]. COPD involves remodeling of the lungs characterized by emphysematous destruction of the alveoli coupled with airway wall thickening. The extent of airway wall thickening is associated with disease progression[3] and this thickening is the major cause of decreased lung function in COPD as remodeling reduces airflow and distensibility[4]. Thickening of the epithelium, greater airway smooth muscle bulk and increased extracellular matrix (ECM) deposition are key structural changes of the remodeled airway wall[4].

The ECM is an acelluar scaffold that surrounds cells and tissues and influences cellular processes such as proliferation, migration, repair and inflammation[5]. As the ECM is involved in many functional processes, any alterations in lung ECM may precipitate changes resulting in airway remodeling.

Lung matrix is predominantly deposited by fibroblasts, which have been shown to contribute to airway remodeling in other airway diseases, such as asthma, by up regulating matrix deposition[6] and increasing cytokine release[7].

The main cause of COPD is chronic particulate exposure, most commonly cigarette smoke[8]. The

emphysematous destruction seen in the lungs of smokers is most likely due to the cytotoxic and pro-inflammatory activity of cigarette smoke[9], however whether cigarette smoke can directly cause remodeling is unknown.

We aimed to examine whether cigarette smoke extract alters the ECM deposited by primary human lung fibroblasts, and if smoke-induced ECM can alter proliferation and cytokine release. We also investigated whether the release of pro-fibrotic cytokines from fibroblasts was increased by cigarette smoke extract.

Exploring the process by which cigarette smoke may cause airway remodeling may yield new therapeutic targets by which airway remodeling may be prevented in COPD and other chronic diseases of the lung.

Methods:

Chemicals

The following chemicals were obtained from the companies indicated:

DMEM, dimethyl sulfoxide (DMSO), BSA, ammonium hydroxide, Direct Red 80, Picric Acid (Sigma, St Louis, MI), PBS, penicillin, streptomycin, amphotericin B (Invitrogen, Carslbad, CA), LY294002, BMS-345541, pyridone-6 (Calbiochem, San Diego, CA), SP60012 (A.G Scientific, San Deigo, CA) FBS (JRH Biosciences, Melbourne, Australia).

Cell Culture

Approval for all experiments with human lung was provided by the Human Ethics Committees of the University of Sydney and the Sydney South West Area Health Service. Human lung fibroblasts were isolated from lung tissue obtained from donors undergoing resection for thoracic malignancies or lung transplantation and they gave written, informed consent. Comparisons of available donor characteristics from the COPD (n=14) and non COPD (n=19) groups are provided in Table 1. The available clinical characteristics of all donors, including age, number of smokers, pack years and forced expiratory volume in 1 s, are provided in Table E1. Methods for isolation of human lung fibroblasts are provided in the online supplement.

Cigarette smoke extract preparation

Cigarette smoke extract was prepared fresh by bubbling smoke from 1 filtered high-tar commercial cigarette at a constant rate through 25ml DMEM[10]. This solution (100% CSE) was then diluted in 0.1% (vol/vol) FBS/Antibiotic/DMEM and applied to cells within 30 minutes of preparation.

Fibroblasts were incubated with 0.5% and 5% CSE in 0.1% (vol/vol) FBS/Antibiotic/DMEM for 72 hours before supernatants were collected and extracellular matrix was exposed. Smoke exposed and smoke naïve plates were incubated in separate, isolated incubators to prevent smoke extract 'leaching' across into naïve plates.

Cytokine Stimulation

In addition to CSE exposure, in some experiments cells were stimulated with 200pM recombinant human TGF-β_1 (R&D Systems, Minneapolis, MN) as a positive control.

Extracellular Matrix ELISA

Deposition of proteins into the extracellular matrix was measured by ELISA using mouse anti-fibronectin C-terminal (Chemicon, Billerica, MA), mouse anti-perlecan (Zymed, Carlsbad, CA), rat anti-laminin β1, mouse anti-collagen V(Abcam, Cambridge, MA), mouse anti-tenascin, mouse anti-collagen IV, mouse anti-elastin, mouse anti-collagen I, mouse anti-collagen III (Sigma) and mouse anti-versican (R&D Systems) antibodies at 1:500 dilution in 1%BSA/PBS. Full details of this method is available in the online supplement.

Picroscirius red assay

Deposition of total fibrillar collagen was measured using a modified picroscirius red assay[11]. Full details of this method is available in the online supplement.

Signaling inhibition

Quiesced fibroblasts were incubated in the presence of SP600125 (10μM), BMS-345541 (30μM), Pyridone-6 (65nM), or LY294002 (3μM) in appropriate concentrations of DMSO in 0.1% FBS/antibiotics/DMEM. After 1 hour, media was aspirated before the addition of 0.5%, 5% CSE or TGF-β_1 (5ng/ml) in the presence of inhibitors for 72 hours.

IL-6, IL-8 and IL-13 Capture ELISA

Levels of IL-6, IL-8 and IL-13 released into the supernatant were assessed using commercial antibody kits according to the manufacturer's instructions (R&D Systems).

Matrix re-seeding

To determine if ECM deposited by fibroblasts under different stimulation altered cellular proliferation, fibroblasts were re-seeded on top of exposed matrix at a density of $0.5x10^4$ cells/ml in 0.1% FBS/Antibiotics/DMEM and incubated without stimulation for 72 hours, whereby supernatant was collected and viable cells were manually counted.

Data Analysis

All analysis was performed using GraphPad Prism 5.0 software (GraphPad Software, La Jolla, CA), Full details are available in the online supplement. Differences were considered significant when $p \leq 0.05$.

Results:

Cigarette smoke extract upregulates fibronectin deposition in COPD fibroblasts via the NF-κB pathway.

To ensure that our model of cigarette smoke extract (CSE) was functional, we assessed fibronectin deposition by primary human lung fibroblasts following exposure to CSE, using transforming growth factor (TGF)-β_1 as a positive control.

Exposure to CSE significantly upregulated fibronectin deposition from fibroblasts obtained from lung samples from donors with COPD ($p<0.05$, n=6) (Figure 1). In contrast, fibroblasts obtained from donors with non-COPD lung disease did not increase fibronectin deposition following 5% CSE exposure (Figure 1).

The increase of fibronectin deposition by CSE in COPD fibroblasts was significantly attenuated by the addition of the NF-κB inhibitor BMS-345541 ($p<0.01$, n=5) (Figure 2). TGF-β_1 induced fibronectin deposition was not significantly altered by BMS-345541 (Figure E-3A, online supplement).

The addition of the c-Jun N-terminal kinase (JNK) inhibitor SP600125, signal transduction and activator of transcription (STAT)-1/3 inhibitor Pyridone-6 and phosphoinositide 3-kinase (PI3K) inhibitor LY294002 did not alter TGF-β_1 or CSE induced fibronectin deposition (Figure E-3A, online supplement).

CSE exposure upregulates perlecan deposition only in COPD fibroblasts via the JAK/STAT pathway.

To examine if other extracellular matrix proteins were altered by CSE, we also assessed the expression of perlecan in the deposited matrices and found that TGF-β_1 and CSE significantly upregulated perlecan deposition in fibroblasts obtained from COPD donors ($p<0.05$, n=5) (Figure 3 A). Surprisingly, whilst TGF-β_1 induced the deposition of perlecan in non-COPD fibroblasts ($p<0.05$, n=4) (Figure 3 B), CSE did not. CSE induced perlecan deposition was partially attenuated by the addition of Pyridone 6 ($p<0.05$, n=5)(Figure 4 A). TGF-β_1 induced perlecan deposition was also partially attenuated by Pyridone-6, however this difference was not statistically significant (Figure E-3B, online supplement). In comparison to fibronectin (Figure 2), the addition of BMS-345541 did not alter CSE induced deposition of perlecan (Figure 4 B). The addition of LY294002 or SP600125 had no effect on CSE or TGF-β_1 induced perlecan deposition (Figure E-3B, online supplement).

CSE does not alter deposition of fibrillar collagen

We did not observe any changes in the deposition of laminin, elastin, tenascin, collagen I, collagen III, collagen IV, collagen V, or versican (data not shown).

To demonstrate that the fibroblasts used in this study could indeed synthesise collagens, we then measured total fibrillar collagen using a modified picroscirius red assay.

Whilst we did not observe an increase in collagen I deposition, TGF-β significantly upregulated deposition of total fibrillar collagen from both COPD and non-COPD fibroblasts (Figure 5). Exposure to CSE did not alter total fibrillar collagen in either group.

Cytokine synthesis is enhanced in COPD fibroblasts

To investigate the effect of CSE on cytokine release, supernatants were collected following 72 hours stimulation and cytokine levels were analyzed by ELISA. Production of IL-8 was increased following 5% CSE stimulation. Interestingly, fibroblasts obtained from COPD donors expressed a significantly greater amount of IL-8 following 5% CSE stimulation (vs non COPD $p<0.01$, n=5,7) (Figure 6). This increase in IL-8 production was attenuated by in the presence of BMS-345541 (vs vehicle control $p<0.05$, n=4) (Figure E1, online supplement).
IL-13 was not detected in the supernatants of fibroblasts at baseline or following stimulation (n=12) (Data not shown).

Deposition of fibronectin and perlecan is the same from fibroblasts obtained from central or peripheral airways

To see if there was any differential matrix production from fibroblasts obtained from different sites in the lungs, we obtained fibroblasts from central and peripheral small airways of the same donors and then stimulated for 72 hours with 5ng/ml TGF-β_1 and 5% CSE.
Deposition of the ECM proteins fibronectin and perlecan was upregulated by both TGF-β_1 and 5% CSE to the same extent in both cell types (Figure E2, online supplement)

Matrix deposited under CSE exposure is pro-proliferative
We examined the effect of re-seeding smoke naïve fibroblasts, onto matrix deposited by fibroblasts under CSE stimulation, to assess whether the matrix was functionally altered.
There was a significantly greater number of fibroblasts after 72 hours incubation on matrix deposited under 5% CSE stimulation (Figure 7 A) (n=12 matrix, 28 fibroblasts, $p<0.05$) whereby the number of fibroblasts was approximately 2 fold greater than compared to those seeded upon matrix deposited under control conditions.
When data was separated into disease state of the donor cells responsible for depositing the matrix, there was an apparent but non-significant trend for higher cell counts on matrices deposited by smoke stimulated COPD fibroblasts (Figure 7 B) as compared to smoke stimulated non-COPD fibroblasts.

Matrix deposited under CSE exposure does not influence cytokine production.
After determining that deposited matrix affected proliferation, we then examined whether matrix deposited under stimulation would alter the production of the cytokines IL-6 and IL-8 from re-seeded fibroblasts. Matrix deposited by fibroblasts under 5% CSE stimulation appeared to reduce release of IL-6 from re-seeded stimuli naïve fibroblasts (Figure 8 A) when compared to matrix deposited from unstimulated non-COPD fibroblasts. COPD matrices had no effect on IL-6 release regardless of stimuli conditions.
There was no significant alteration in IL-8 release from stimuli naïve fibroblasts reseeded on matrices from either COPD or Non COPD matrices (Figure 8 B). Stimuli naïve fibroblasts tended to have a 200pg/ml greater IL-8 release when seeded on COPD matrices as compared to when seeded on non-COPD matrices however this difference was not statistically significant.

Discussion
This study has demonstrated that human lung fibroblasts obtained from donors with COPD are more responsive to CSE and produce pro-fibrotic cytokines more readily than non-COPD donors. In addition, we have shown that CSE directly activates the NF-κB pathway. We have also demonstrated that the ECM produced by lung fibroblasts following exposure to CSE is functionally altered, having pro-proliferative characteristics.

We demonstrated *in vitro* that by up regulating deposition of ECM proteins and cytokines from lung fibroblasts, CSE exposure may directly influence airway remodeling. As the ECM is involved in processes of cellular proliferation and angiogenesis, and various ECM proteins have been demonstrated to be upregulated in lungs of patients with COPD[12,13], it is rational to conclude that the functional alterations of the ECM may be relevant *in vivo.*
Matrix produced by fibroblasts following CSE exposure is pro-proliferative. The pro-proliferative effects of the CSE induced matrix were unexpected as previous research has shown

that direct exposure of CSE to fibroblasts inhibits proliferation[14]. The role of the extracellular matrix in affecting cellular proliferation, migration and differentiation is well known[5]. Fibronectin can have pro-proliferative activity on human lung carcinoma cell growth via suppression of the p21 pathway[15]. As 5% CSE increased fibronectin deposition into the matrix, we speculate that the pro-proliferative actions of smoke induced matrix on human lung fibroblasts may be due to this increased fibronectin.

Perlecan, a heparan sulfate proteoglycan, can store and protect growth factors such as members of the fibroblast growth factor (FGF) family[16]. Perlecan expression has been linked to tumor growth and angiogenesis[17]. Reducing perlecan synthesis with a perlecan antisense cDNA construct decreases proliferation and migration of cancer cells *in vitro*[18]. Thus the observed increase in perlecan and fibronectin deposition from COPD fibroblasts following CSE exposure may increase cellular proliferation and angiogenesis in the lungs, which in turn may cause irreversible airway remodeling. Additionally, the presence of perlecan is increased in damaged tissue that undergoes mechanical strain, such as cardiac tissue[19] and the presence of perlecan is also involved in the formation of proper basement membranes[20], so the upregulation of perlecan from lung tissue may also combat strain induced by hyperinflation of the alveolar airspaces in emphysema.

Thus we hypothesize that a functionally altered ECM may perpetuate the pathophysiology of COPD in the absence of stimulation. The extent and duration for which the matrix remains functionally altered requires investigation, but may provide insight into the mechanisms by which decreased lung function never completely recovers in patients with COPD who have quit smoking[21,22].

It has been previously described that fibronectin deposition from human lung fibroblasts following cigarette smoke exposure is due to the JNK and MAPK pathways[23], whilst the addition of inhibitors to these signaling molecules did not result in a statistically significant attenuation of CSE effects, a trend was observed. Our data compliments and extends previous work by demonstrating the role of the NF-κB pathway in smoke induced fibronectin deposition. This pathway may also be more readily activated in COPD as seen by increased IL-8 release in response to cigarette smoke extract exposure. We also demonstrated that perlecan and fibronectin are produced by different signaling pathways in response to CSE stimulation. This was not unexpected as CSE is composed of many different chemicals which can activate multiple pathways, however these findings highlight the fact that fibroblasts may produce different matrix proteins depending on external stimulation.

We are the first to show that smoke induced deposition of perlecan from COPD fibroblasts may be due to STAT-1/3 activation. It is reasonable to suggest that activation of this pathway may occur at a lower threshold/more easily in cells from donors with COPD, thus we see deposition of ECM proteins in response to smoke exposure as well as changes in proliferation and increased IL-8 release. This is supported by recent work showing increased activation of MAPK in the lungs of COPD patients[24.] Further investigation of the role of STAT activation in COPD is warranted.

As fibroblasts are situated in the submucosal layer of the lungs, it is appropriate to use cigarette smoke extract as any chemicals that diffuse across the epithelial layer will be in a soluble form. Our study demonstrated that the location which the fibroblasts were derived from did not affect the response to cigarette smoke.

Cigarette smoke is composed of over 4000 different chemicals and the exact mediator for the changes in ECM in both composition and function is not known. Nicotine has been shown to induce fibronectin deposition in a dose-dependant manner[23], and it is known that molecules which cause oxidative stress such as hydrogen peroxide are found in greater levels in the lungs of patients with COPD[24] and can activate intracellular signaling molecules[26]. It is likely that a combination of smoke-derived molecules and activation of multiple signaling

pathways underlie processes by which ECM deposition is upregulated. As inhibiting signaling molecules had different effects on CSE and TGF-β_1 induced ECM deposition, it is likely that CSE and TGF-β_1 involve different signaling mechanisms to upregulate ECM protein deposition.

The COPD fibroblasts came from donors undergoing transplantation for severe, end-stage COPD and required a BODE index score of 7-10 to be eligible for transplantation[27]. Fibroblasts from donors with COPD had increased deposition of fibronectin and perlecan in response to CSE, whereas fibroblasts obtained from donors with non-COPD lung disease did not. This suggests that the lungs of donors with COPD may be primed for remodeling by cigarette smoke exposure. Further studies comparing smokers without COPD, non smokers and smokers with COPD would aid in answering whether altered matrix deposition is a result of prior chronic exposure to cigarette smoke or an underlying phenotype characteristic of COPD.

The non-COPD donor group came from a diverse range of lung diseases (see table E1), the majority of which, such as lung cancer and asthma, can involve airway obstruction and areas of fibrosis. Although cells from these donors responded to TGF-β_1 stimulation, they did not upregulate ECM deposition following CSE stimulation. Thus we can conclude that COPD fibroblasts are altered in such a way as to deposit ECM proteins following CSE stimulation. Pathogenesis of other smoking induced diseases suggests that, although there is a genetic component, the disease pathogenesis is most likely due to alterations resulting from prolonged exposure to cigarette smoke. Genetic variability of individuals may affect the sensitivity of an individual to cigarette smoke induced pathogenesis, but we believe that given enough time and enough exposure, various hallmark characteristics of COPD will appear, to some extent, in all persistent smokers. Therefore we believe that the differential response of the COPD fibroblasts is most likely due to epigenetic reprogramming of genetically susceptible individuals by cigarette smoke.

In conclusion, we have demonstrated for the first time that the ECM produced by fibroblasts following stimulation with CSE is functionally different and cigarette smoke may prime the airways in such a way as to create an environment whereby airway remodeling is encouraged. We have also added data to the growing pool of knowledge whereby differences between cells from donors with COPD and other lung diseases are known. Further research on these differences may result in viable therapeutic targets for reducing the detrimental airway changes underlying COPD.

References:

1) Celli, B. R. and W. MacNee. Standards for the diagnosis and treatment of patients with COPD: a summary of the ATS/ERS position paper. Eur Respir J 2004; 23(6): 932-46.

2) Viegi et al. Definition, epidemiology and natural history of COPD. Eur Respir J 2007; 30(5) 993-1013

3) Hogg, J. C., F. Chu, et al. The nature of small-airway obstruction in chronic obstructive pulmonary disease. N Engl J Med 2004; 350(26): 2645-53.

4) James, A. L. and S. Wenzel. Clinical relevance of airway remodelling in airway diseases. Eur Respir J 2007; 30(1): 134-155

5) Dunsmore, S. E. and D. E. Rannels. Extracellular matrix biology in the lung. Am J Physiol Lung Cell Mol Physiol 1996; 14(1): L3-L27.

6) Lewis, C. C., H. W. Chu, et al. Airway fibroblasts exhibit a synthetic phenotype in severe asthma. J Allergy Clin Immunol 2005; 115(3): 534-540.

7) Bedke, N., Haitchi, H.M., et al. Contribution of bronchial fibroblasts to the antiviral response in asthma. J Immunol 2009; 182: 3660-3667

8) Sethi, J. M. and C. L. Rochester. Smoking and chronic obstructive pulmonary disease. Clinic Chest Med 2000; 21(1): 67-86.

9) Evans, M. D. and W. A. Pryor. Cigarette smoking, emphysema, and damage to alpha 1-proteinase inhibitor. Am J Physiol Lung Cell Mol Physiol 1994; 266(6): L593-611.

10) Mercer, B. A., N. Kolesnikova, et al. Extracellular Regulated Kinase/Mitogen Activated Protein Kinase Is Up-regulated in Pulmonary Emphysema and Mediates Matrix Metalloproteinase-1 Induction by Cigarette Smoke. J. Biol. Chem. 2004; 279(17): 17690-17696.

11) Walsh, B.J., Thornton, S.C., et al. Microplate reader-based quantitation of collagens. Analytical Biochem 1992; 203:187-190

12) Song, W. D., Zhang, A., et al. Fibronectin and hyaluronan in bronchoalveolar lavage fluid from young patients with chronic obstructive pulmonary diseases. Respiration 1995; 62: 125–129

13) Merrilees, M. J., Ching, P. S.T., et al. Changes in elastin, elastin binding protein and versican in alveoli in chronic obstructive pulmonary disease. Resp Res 2008; 9(1):41

14) Nakamura, Y., D. J. Romberger, et al. Cigarette smoke inhibits lung fibroblast proliferation and chemotaxis. Am. J. Respir. Crit. Care Med. 1995; 151(5): 1497-1503.

15) Han, Sidell, & Roman Fibronectin stimulates human lung carcinoma cell proliferation by suppressing p21 gene expression via signals involving Erk and Rho kinase. Cancer lett 2005; 219 71-81

16) Knox, S., J. Melrose, et al. Electrophoretic, biosensor, and bioactivity analyses of perlecans of different cellular origins. Proteomics 2001; 1(12): 1534-1541.

17) Jiang, X. N., H. Multhaupt, et al. Essential contribution of tumor-derived perlecan to epidermal tumor growth and angiogenesis. J Histo Cytochem 2004; 52(12): 1575-1590.

18) Adatia, R., A. Albini, et al. Suppression of invasive behavior of melanoma cells by stable expression of anti-sense perlecan cDNA. Ann Oncol 1997; 8(12): 1257-1261.

19) Sasee, P., Malan, D., et al. Perlecan is critical for heart stability. Cardiovas Res 2008; 80: 435-444

20) Sakai, K., Nakamura, T, et al. Angioinhibitory action of NK4 involves impaired extracellular assembly of fibronectin mediated perlecan-NK4 association. J Biol Chem 2009; 284 (33):22491-99

21) Godtfredsen, Lam et al, COPD-related morbidity and mortality after smoking cessation: status of the evidence. Eur Respir J 2008; 32(4):844-53

22) Gamble, Grootendorst et al, Airway mucosal inflammation in COPD is similar in smokers and ex-smokers: a pooled analysis. Eur Respir J 2007; 30(3)467-71

23) Roman, Ritzenthaler et al. Nicotine and fibronectin expression in lung fibroblasts: implications for tobacco-related lung tissue remodeling, FASEB 2004; 18(12): 1436-38

24) Renda, T., S. Baraldo, et al. Increased activation of p38 MAPK in COPD. Eur Respir J 2008; 31(1): 62-69.

25) Dekhuijzen, P. N. R., K. K. H. Aben, et al. Increased exhalation of hydrogen peroxide in patients with stable and unstable chronic obstructive pulmonary disease. Am J Respir Crit Care Med 1996; 154(3): 813-816.

26) Rao, G. N. Protein tyrosine kinase activity is required for oxidant-induced extracellular signal-regulated protein kinase activation and c-fos and c-jun expression. Cell Sig 1997; 9(2): 181-187.

27) Orens, J.B., Estenne, M., et al. International Guidelines for the Selection of Lung Transplant Candidates: 2006 Update—A Consensus Report From the Pulmonary Scientific Council of the International Society for Heart and Lung Transplantation.
J Heart Lung Transplant 2006; 25:745–55.

28) Johnson, P. R. A., Burgess, J.K., et al. Extracellular matrix proteins modulate asthmatic airway smooth muscle cell proliferation via an autocrine mechanism. J Allergy Clin Immunol 2004; 113(4): 690-696.

Figure 1. Deposition of fibronectin from human lung fibroblasts from patients with COPD (n=6) or non-COPD lung disease (n=7) as measured by ELISA following 72 hours stimulation with 0.5% or 5% cigarette smoke extract (CSE). The TGF-β_1 (5ng/ml) was used as a positive control. Data expressed as absorbance at 405nm. Bar graphs represent mean $\pm$ SEM.*p<0.05 vs unstimulated, 2-way repeated measures ANOVA.

Figure 2. Attenuation of 5% CSE induced fibronectin deposition from COPD human lung fibroblasts by the addition of NF-κB inhibitor BMS-345541 (BMS) as compared to 0.006%(v/v) DMSO (Vehicle control), following 72 hours stimulation with 5% CSE in the presence of 30mM BMS-345541. Data expressed as % of 5%CSE induced fibronectin deposition. Bar graphs represent mean $\pm$ SEM. **p<0.01 vs vehicle control. Student's paired t-test, n=5

Figure 3. Deposition of perlecan from human lung fibroblasts from (A) patients with COPD (n=5) or (B) non-COPD lung disease (n=4) as measured by ELISA following 72 hours stimulation with 0.5% or 5% CSE. The profibrotic cytokine TGF-β_1 (5ng/ml) was used as a positive control. Data expressed as absorbance at 405nm. Bar graphs represent mean ± SEM. *p<0.05 vs unstimulated, repeated measures 1-way ANOVA with dunnets post-test.

Figure 4. Attenuation of 5% CSE induced perlecan deposition from COPD human lung fibroblasts by pyridone-6 (A) but not BMS-345541 (B) as compared to 0.006%(v/v) DMSO (Vehicle control), Data expressed as % of 5%CSE induced perlecan deposition. Bar graphs represent mean ± SEM. **p<0.01 vs vehicle control. Student's paired t-test, n=5

Figure 5 Deposition of total collagen from human lung fibroblasts following stimulation with 0.5 or 5% cigarette smoke extract (CSE), 5ng/ml TGF-β as measured by picroscirius red assay. Data expressed as % of unstimulated control. Bars represent mean, error bars represent SEM. * p<0.05 vs unstimulated control. n=4 for each disease type.

Figure 6. Release of interleukin(IL)-8 from human lung fibroblasts in response to stimulation with 0.5% or 5% CSE, as compared to the positive control TGF-β_1. Data expressed in pg/ml. Bar graphs represent mean ± SEM. **p<0.01 COPD (n=5) vs non-COPD (n=7), 2-way repeated measures ANOVA.

Figure 7. Effect of deposited matrix on proliferation of (A) reseeded primary human lung fibroblasts (n=28,38). Data separated into COPD or non COPD matrix (B) Stimuli naïve cells were plated on top of matrix deposited from fibroblasts stimulated with 0.5% or 5% CSE for 72 hours and viable cells were counted manually. Data were normalized to % of control. Bar graphs represent mean ± SEM. *p<0.05 vs unstimulated. n= 28-38 fibroblasts reseeded on 12 matrices.

Figure 8. Effect of deposited matrix on (A) IL-6 and (B) IL-8 release from re-seeded primary human lung fibroblasts. Stimuli naïve cells were plated on top of matrix deposited from fibroblasts stimulated with 0.5% or 5% CSE for 72 hours and supernatants were collected and analysed for IL-6 and IL-8 release via ELISA. All data represented in pg/ml. Bars represent mean ± SEM. n= 28 fibroblasts reseeded on 6 COPD or 6 non COPD matrices.

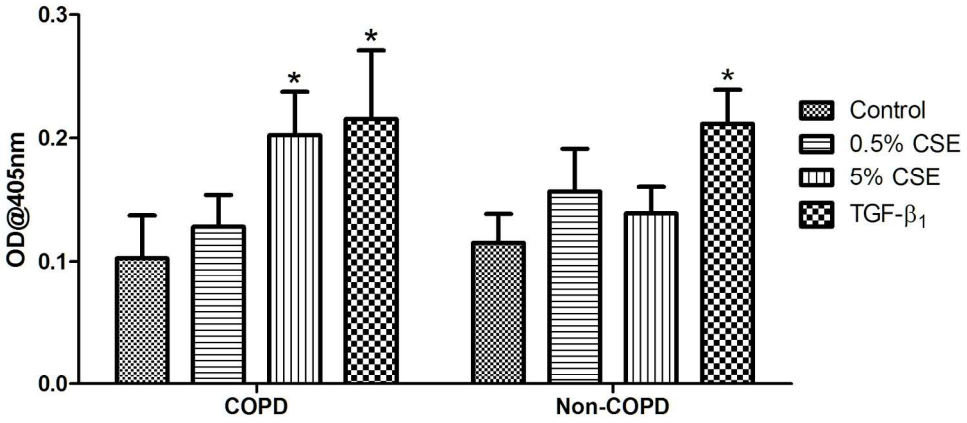

Figure 1. Deposition of fibronectin from human lung fibroblasts from patients with COPD (n=6) or non-COPD lung disease (n=7) as measured by ELISA following 72 hours stimulation with 0.5% or 5% cigarette smoke extract (CSE). The TGF-β1 (5ng/ml) was used as a positive control. Data expressed as absorbance at 405nm. Bar graphs represent mean + SEM.*p<0.05 vs unstimulated, 2-way repeated measures ANOVA.
174x87mm (300 x 300 DPI)

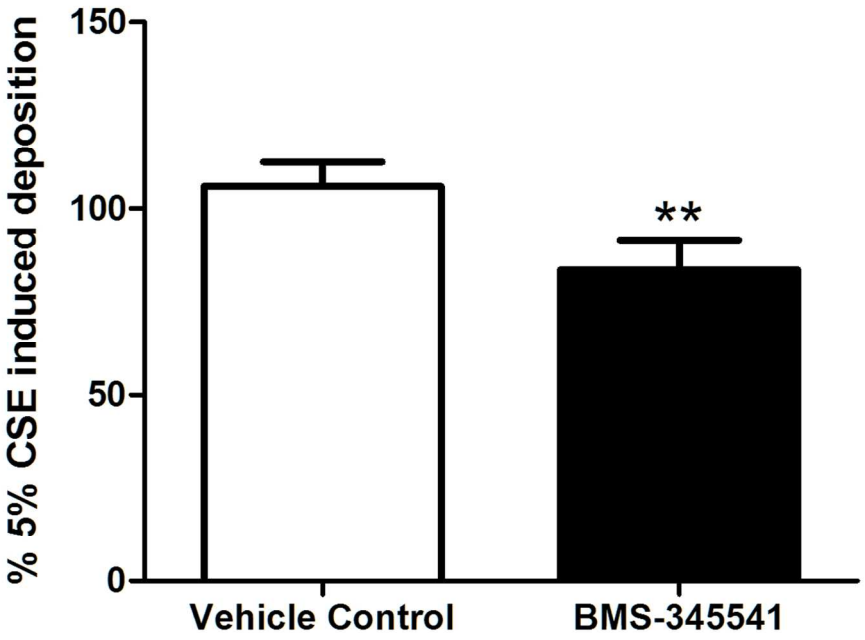

Figure 2. Attenuation of 5% CSE induced fibronectin deposition from COPD human lung fibroblasts by the addition of NF-κB inhibitor BMS-345541 (BMS) as compared to 0.006%(v/v) DMSO (Vehicle control), following 72 hours stimulation with 5% CSE in the presence of 30mM BMS-345541. Data expressed as % of 5%CSE induced fibronectin deposition. Bar graphs represent mean + SEM. **p<0.01 vs vehicle control. Student's paired t-test, n=5
106x82mm (300 x 300 DPI)

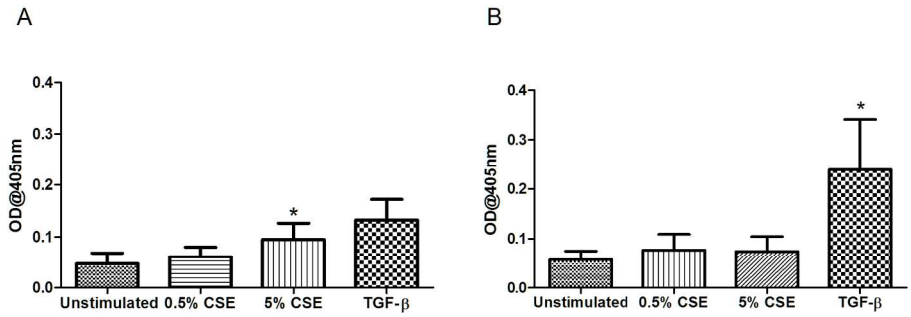

Figure 3. Deposition of perlecan from human lung fibroblasts from (A) patients with COPD (n=5) or (B) non-COPD lung disease (n=4) as measured by ELISA following 72 hours stimulation with 0.5% or 5% CSE. The profibrotic cytokine TGF-β1 (5ng/ml) was used as a positive control. Data expressed as absorbance at 405nm. Bar graphs represent mean + SEM. *p<0.05 vs unstimulated, repeated measures 1-way ANOVA with dunnets post-test.
179x65mm (300 x 300 DPI)

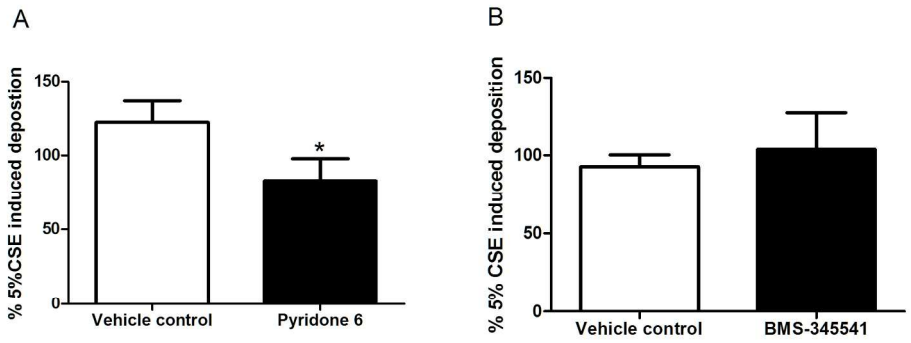

Figure 4. Attenuation of 5% CSE induced perlecan deposition from COPD human lung fibroblasts by pyridone-6 (A) but not BMS-345541 (B) as compared to 0.006%(v/v) DMSO (Vehicle control), Data expressed as % of 5%CSE induced perlecan deposition. Bar graphs represent mean + SEM. **p<0.01 vs vehicle control. Student's paired t-test, n=5
198x82mm (300 x 300 DPI)

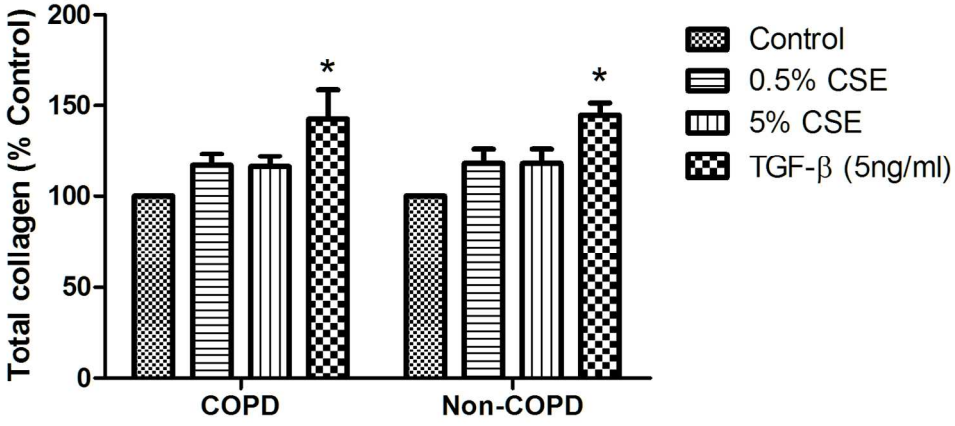

Figure 5 Deposition of total collagen from human lung fibroblasts following stimulation with 0.5 or 5% cigarette smoke extract (CSE), 5ng/ml TGF-β as measured by picroscirius red assay. Data expressed as % of unstimulated control. Bars represent mean, error bars represent SEM. * $p<0.05$ vs unstimulated control. n=4 for each disease type.
139x67mm (300 x 300 DPI)

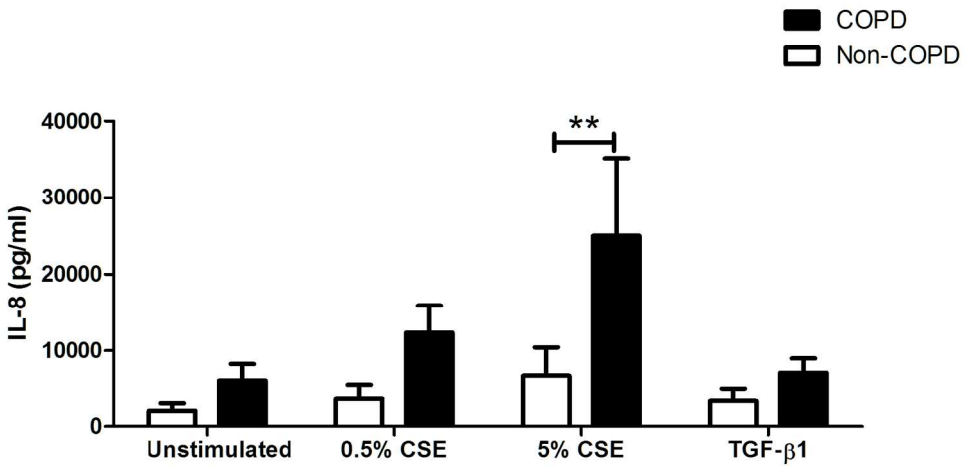

Figure 6. Release of interleukin(IL)-8 from human lung fibroblasts in response to stimulation with 0.5% or 5% CSE, as compared to the positive control TGF-β1. Data expressed in pg/ml. Bar graphs represent mean + SEM. **p<0.01 COPD (n=5) vs non-COPD (n=7), 2-way repeated measures ANOVA.
166x88mm (300 x 300 DPI)

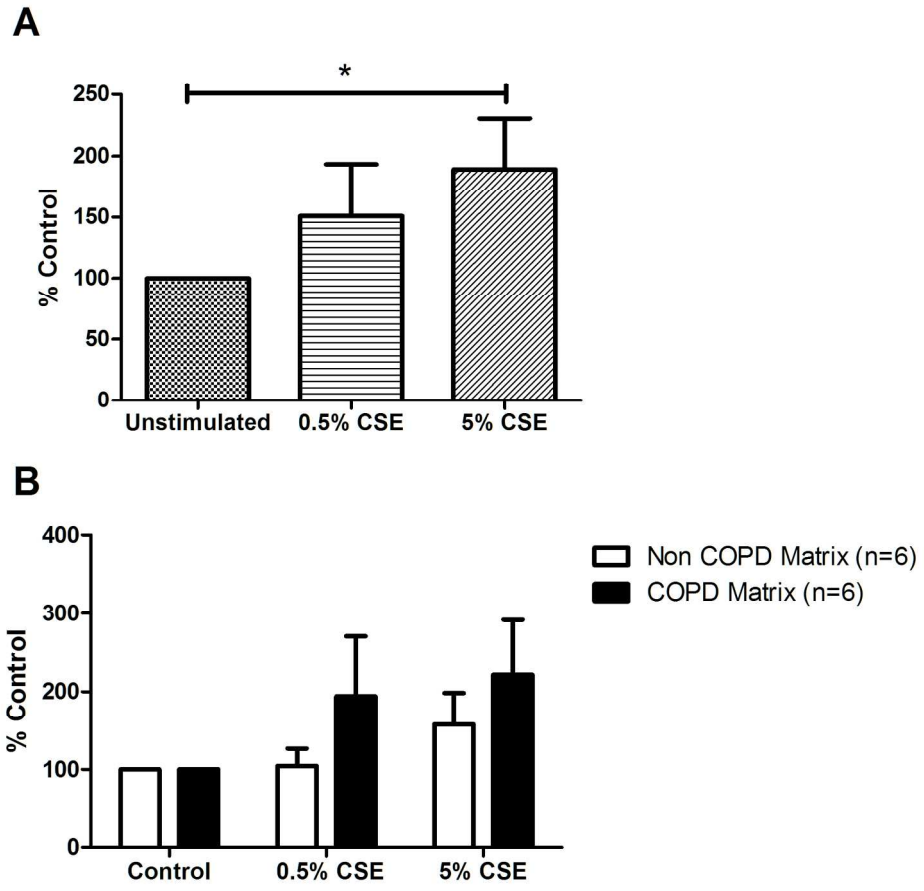

Figure 7. Effect of deposited matrix on proliferation of (A) reseeded primary human lung fibroblasts (n=28,38). Data separated into COPD or non COPD matrix (B) Stimuli naïve cells were plated on top of matrix deposited from fibroblasts stimulated with 0.5% or 5% CSE for 72 hours and viable cells were counted manually. Data were normalized to % of control. Bar graphs represent mean + SEM. *p<0.05 vs unstimulated. n= 28-38 fibroblasts reseeded on 12 matrices.
181x171mm (300 x 300 DPI)

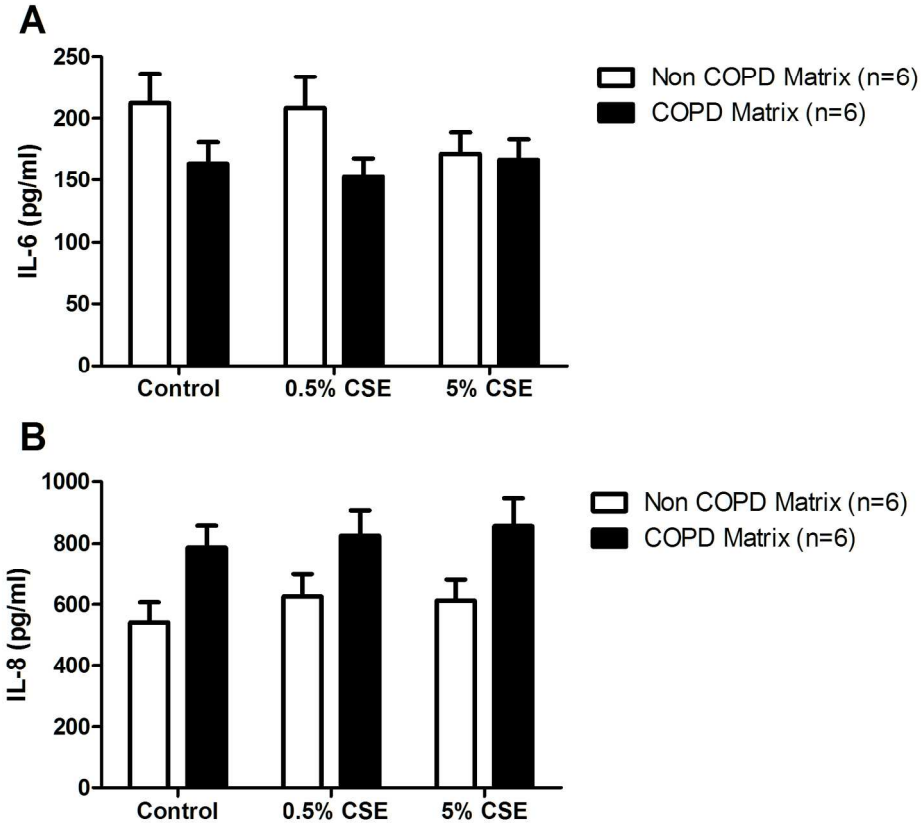

Figure 8. Effect of deposited matrix on (A) IL-6 and (B) IL-8 release from re-seeded primary human lung fibroblasts. Stimuli naïve cells were plated on top of matrix deposited from fibroblasts stimulated with 0.5% or 5% CSE for 72 hours and supernatants were collected and analysed for IL-6 and IL-8 release via ELISA. All data represented in pg/ml. Bars represent mean + SEM. n= 28 fibroblasts reseeded on 6 COPD or 6 non COPD matrices.
183x162mm (300 x 300 DPI)

Data supplement

MATRIX PROTEINS FROM SMOKE EXPOSED FIBROBLASTS ARE PRO-PROLIFERATIVE

David I Krimmer[1,2 *], Janette K Burgess[1,2] , Teh K Wooi[1,2], Judith L Black[1,2] & Brian GG Oliver[1,2]

Donor #	Age (years)	Gender	Disease	Surgery	Smoking	FEV1(%Pred)	FVC(%Pred)	FEV1:FVC	Experiment
1	54	F	COPD	R	ex	73	93	0.62	4
2	51	F	COPD	T	ex	20	58	0.28	4
3	56	F	COPD	T	ex	29	66	0.37	1,2,3,5
4	42	M	COPD	T	ex	14	65	0.16	4,5
5	56	M	COPD	T	ex	14	35	0.31	1,2,3,5
6	40	M	COPD	T	ex	27	51	0.72	1,2,3,5
7	59	M	COPD	T	ex	11	52	0.16	5
8	54	M	COPD	T	ex	62	64	0.74	5
9	73	M	COPD	R	ex	67	73	0.73	5
10	41	M	COPD	T	ex	23	20	0.79	5
11	69	M	COPD	T	ex	56	59	0.74	5
12	61	M	COPD	T	ex	13	47	0.24	1,2
13	63	M	COPD	T	ex	22	79	0.23	1,2,3
14	61	M	COPD	T	ex	18	59	0.24	1,2
15	69	M	NSCLC	R	ex	N/A	N/A	N/A	4
16	39	M	asthma	B	no	89	91	0.8	5
17	59	F	Ca	R	no	93	97	0.91	5
18	73	M	NSCLC	R	ex	63	55	0.92	5
19	60	M	Bronchiectasis	T	N/A	22	34	0.51	5
20	61	M	Ca	R	ex	112	118	0.75	5
21	79	F	NSCLC	R	ex	88	99	0.72	1,2,3,5
22	71	M	NSCLC	R	no	93	89	0.79	5
23	72	M	NSCLC	R	ex	83	89	0.71	5
24	64	M	Ca	R	ex	93	95	0.77	5
25	66	M	NSCLC	R	ex	91	98	0.71	5
26	37	M	NSCLC	R	ex	103	101	0.79	5
27	63	F	NSCLC	R	no	61	57	0.88	1,2,3
28	63	M	Ca	R	ex	79	71	0.86	1,2,3
29	21	M	Chronic rejection	T	no	20	26	0.69	1,2
30	15	M	PPHT	T	no	78	87	0.82	1,2
31	36	F	PPHT	T	no	85	98	0.73	1,2,3
32	33	F	LAM	T	no	N/A	N/A	N/A	1
33	48	M	Ca	R	ex	88	93	0.75	2

Table E-1 Donor characteristics. $FEV_{1:}$ Forced expiratory volume in 1 second % predicted, FVC: Forced vital capacity % predicted. Disease; NSCLC: Non small-cell lung cancer, Ca: Cancer (unspecified), PPHT: Primary pulmonary hypertension, LAM: Lymphangioleiomyomatosis. Reasons for surgery; R: Tissue resection, T: lung transplant, B: Biopsy. Experiments; 1: ECM production, 2: Cytokine production, 3: Total collagen deposition, 4: Central vs Peripheral fibroblast, 5: Reseeding assay.

Isolation of human lung fibroblasts

Briefly, cells were obtained from proximal lung tissue containing small airways (<1mm) which were deemed to be free of tumour following pathological examination. This tissue was minced in 1-2mm pieces into sterile Hanks Buffered Saline Solution (Hanks) and centrifuged for 5 minutes at 1000rpm. Supernatant was aspirated and the tissue pellet was resuspended and plated onto tissue culture grade plastic flasks in 10% (vol/vol) FBS/2% antibiotics/DMEM.

To obtain central fibroblasts, a section of bronchi ~10mm diameter was isolated from the lung tissue. This was washed briefly in 70% ethanol followed by 3 changes of sterile Hanks solution. The epithelial layer was manually removed, followed by blunt dissection of airway smooth muscle bundles out of the section. The remaining tissue was then minced into 1-2mm fragments and added to tissue culture flasks as described above.

All experiments were carried out using cells between passage 3 and 6.

Exposure of deposited extracellular matrix

Matrix deposited from stimulated fibroblasts was exposed following supernatant collection as previously described[28]. Cells were washed with sterile PBS, then incubated for 15 minutes at 37^{o}C in the presence of sterile 16mM ammonium hydroxide. Following aspiration, the cell free matrix was washed 3 times with sterile PBS to remove ammonium hydroxide and cell debris.

Extracellular matrix ELISA Protocol

Plates were defrosted to room temperature. PBS was aspirated and plates were washed once in 0.05% (vol/vol) Tween-20/PBS (T-PBS). Non-specific binding was removed by blocking for 2 hours with 1% BSA/PBS with agitation. Following 2x washes in T-PBS, detection antibody was added overnight at 4^{o}C at 50µl/well at a dilution of 1:500 in 1%BSA/T-PBS. Biotinylated secondary antibody was added after 3x washes in T-PBS at 1:500 in 1% BSA/T-PBS for 2 hours at room temperature with agitation. Following an additional 3x washes in T-PBS, 50µl/well streptavidin-HRP was added at 1:200 in 1% BSA/T-PBS. Plates were washed a final 3x with T-PBS before incubation with 50µl/well ABTS substrate for 20 minutes at room temperature in the dark. The reaction was stopped by the addition of 50µl/well 1M $NaHPO_3$ and absorbance was measured at 405nm using a Wallac-1000 plate reader and software.

In preparation for *in vitro* experimentation, cells were seeded in 96 &/or 12 well plates for 72 hours in 5% (vol/vol) FBS/antibiotics/DMEM at a density of $1x10^4$ cells/cm^2. Cells were equilibrated before experimental stimulation for 24 hours in 0.1% (vol/vol) FBS/antibiotics/DMEM.

Picroscirius red assay

To assess alterations in total fibrillar collagen deposition from human lung fibroblasts, we used a previously published modified picroscirius red assay[11]. Previously prepared plates were defrosted to room temperature. PBS was aspirated and plates were washed once in 0.05% (vol/vol) Tween-20/PBS (T-PBS). 50µl of 0.1%(w/v) scirius red solution was added

and plates were incubated for 1 hour at room temperature. Following 5x washes in 10mM HCL, plates were then incubated for 5 minutes with 0.1M NaOH, before the solution was transferred into new plates and absorbance was measured at 540nm using a Wallac-1000 plate reader and software.

Data were analyzed for normality using Kolmogorov-Smirnov and D'Agostino & Pearson omnibus normality tests. ECM proteins and cytokine expression in fibroblasts following smoke and cytokine stimulation was analysed using 1-way repeated measures ANOVA with Dunnets post-test comparing stimulation vs unstimulated. Comparisons between inhibitors of signaling molecules and DMSO vehicle controls were made using paired Students t-tests.

Figure E1. Attenuation of CSE induced IL-8 release from COPD fibroblasts by the addition of BMS-345541 as compared to 0.006%(V/V) DMSO (Vehicle control). Data expressed as % of 5% CSE induced IL-8 release. Bar graphs represent mean ± SEM.*p<0.05 vs vehicle control, n=4

Figure E2. Deposition of fibronectin (A) and perlecan (B) is upregulated by TGF-β_1 and 5% CSE in both central and peripheral lung fibroblasts derived from the same donors. Data expressed as % of unstimulated control. Bar graphs represent mean ± SEM. n=4

Figure E3. Attenuation of TGF-β_1 and 5% CSE induced fibronectin (A) and perlecan (B) deposition from COPD fibroblasts following inhibition of NF-kB (BMS-345541), JNK (SP600125), STAT 1/3 (Pyridone 6) and PI3K (LY294002) signalling molecules. Data analyzed by two-tailed student's T-test. Bar graphs represent mean ± SEM. n=5

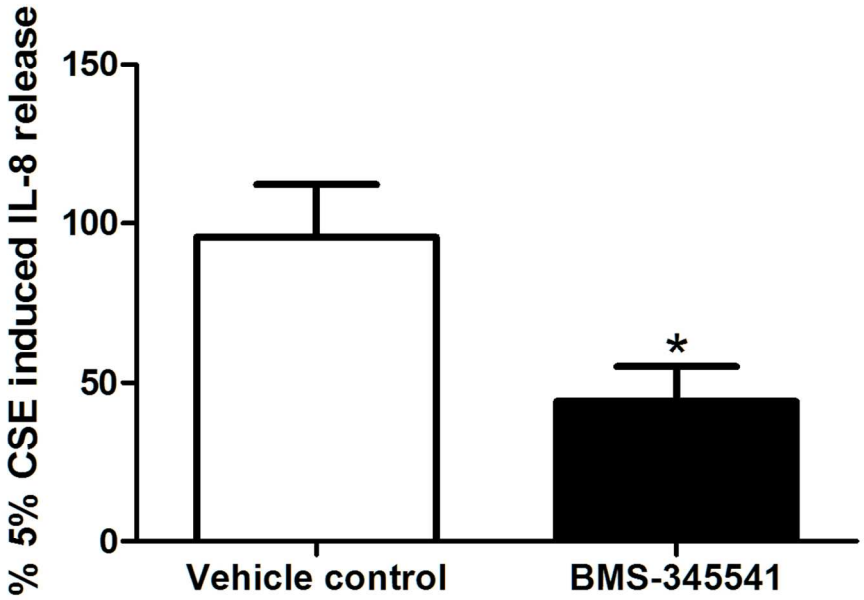

Figure E1. Attenuation of CSE induced IL-8 release from COPD fibroblasts by the addition of BMS-345541 as compared to 0.006%(V/V) DMSO (Vehicle control). Data expressed as % of 5% CSE induced IL-8 release. Bar graphs represent mean + SEM.*p<0.05 vs vehicle control, n=4
105x69mm (300 x 300 DPI)

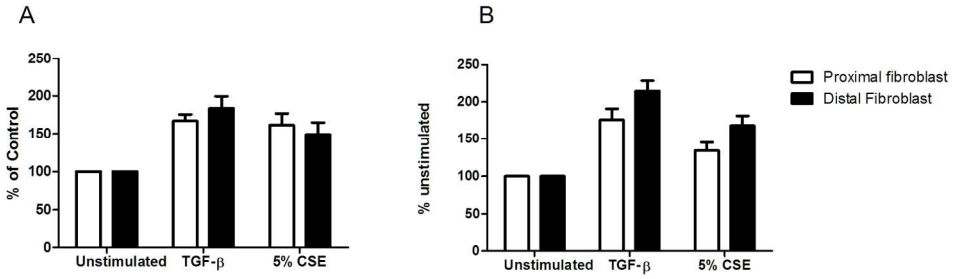

Figure E2. Deposition of fibronectin (A) and perlecan (B) is upregulated by TGF-β1 and 5% CSE in both central and peripheral lung fibroblasts derived from the same donors. Data expressed as % of unstimulated control. Bar graphs represent mean + SEM. n=4
176x57mm (300 x 300 DPI)

A

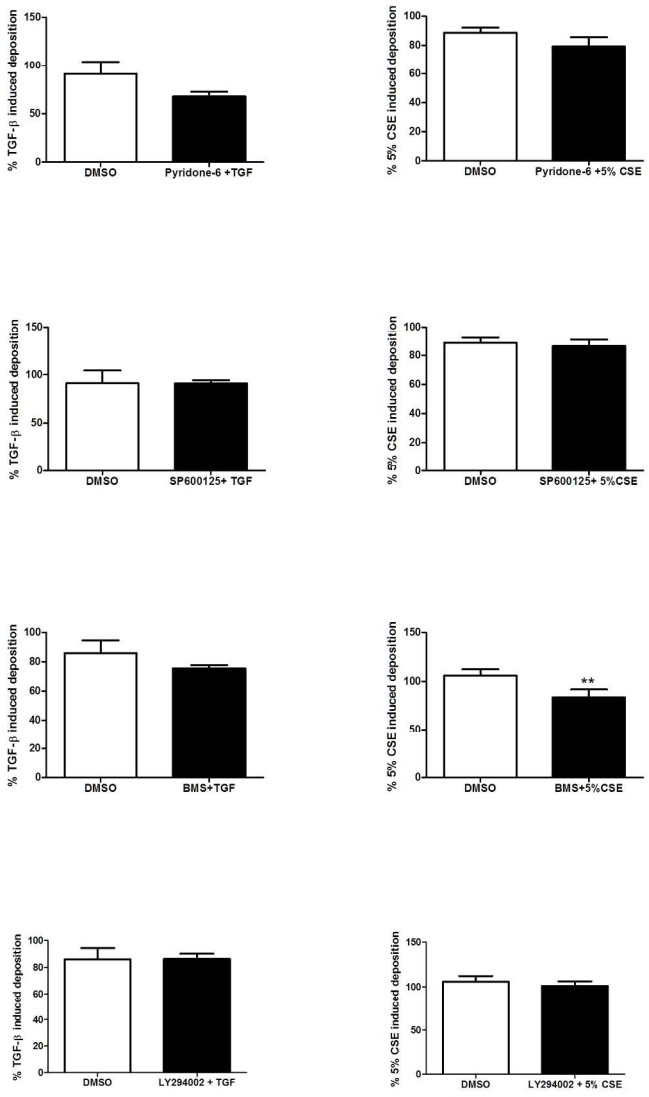

Figure E3. Attenuation of TGF-β1 and 5% CSE induced fibronectin (A) and perlecan (B) deposition from COPD fibroblasts following inhibition of NF-kB (BMS-345541), JNK (SP600125), STAT 1/3 (Pyridone 6) and PI3K (LY294002) signalling molecules. Data analyzed by two-tailed student's T-test. Bar graphs represent mean + SEM. n=5
154x256mm (300 x 300 DPI)

B

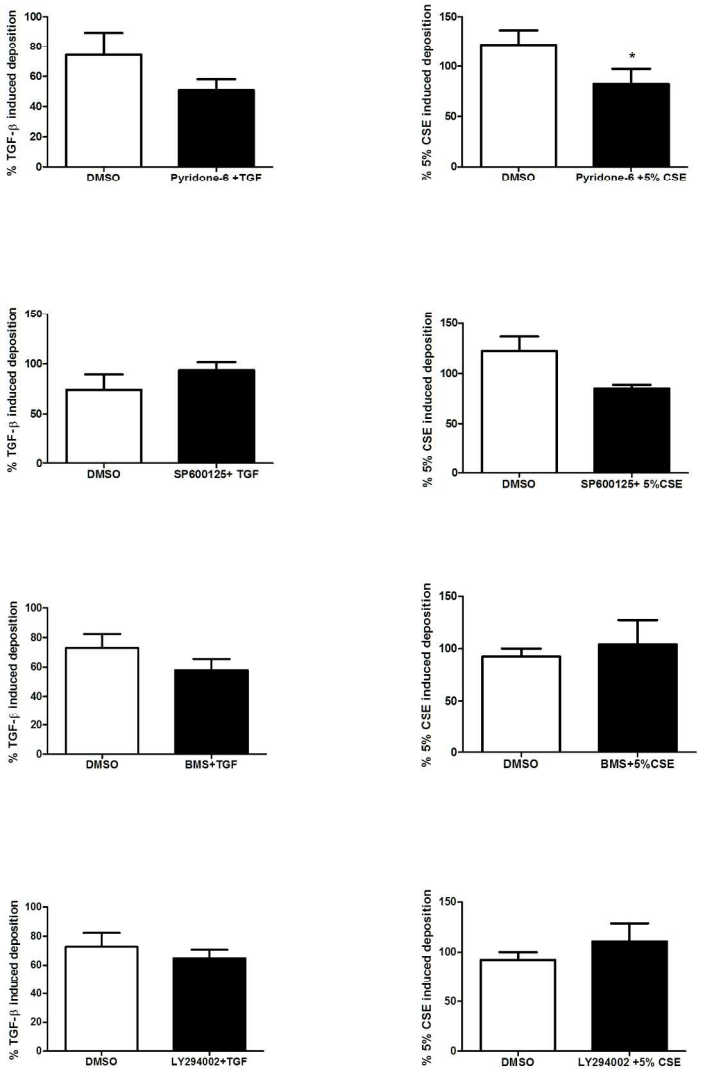

Figure E3. Attenuation of TGF-β1 and 5% CSE induced fibronectin (A) and perlecan (B) deposition from COPD fibroblasts following inhibition of NF-kB (BMS-345541), JNK (SP600125), STAT 1/3 (Pyridone 6) and PI3K (LY294002) signalling molecules. Data analyzed by two-tailed student's T-test. Bar graphs represent mean + SEM. n=5
162x250mm (300 x 300 DPI)